34th Annual International Conference of the IEEE EMBS
San Diego, California USA, 28 August - 1 September, 2012

High-Throughput Spectral System for Interrogation of Dermally-Implanted Luminescent Sensors

Ruiqi Long and Mike McShane, *Senior Member, IEEE*

***Abstract*—Ratiometric luminescent microparticle sensors have been developed for sensing biochemical targets such as glucose in interstitial fluid, enabling use of dermal implants for on-demand monitoring. For these sensor systems to be deployed *in vivo*, a matched optoelectronic system for interrogation of dermally-implanted sensors was previously designed, constructed, and evaluated experimentally. During evaluation experiments, it revealed that the system efficiency was compromised by losses due to fiber connections of a commercial spectrometer. In this work, a high-throughput spectral system was presented to solve the photon loss problem. This system was designed, constructed, and tested. The throughput was around hundred time more than the previous system we used, and it was cost-effective, as well. It enables use of an integrated system for excitation, collection and measurement of luminescent emission, and will be used as a tool for *in vivo* studies with animal models or human subjects.**

I. Introduction

A. Background

Among various "minimally-invasive" biosensors, a combination of fiber optic technology and highly sensitive luminescent transduction chemistry has shown particular promise [1-3]. These sensor systems generally employ a probe composed of a luminescent chemical assay immobilized within a selective-permeable membrane at the tip of an optical fiber, and signals are transmitted through optical fibers. However, fiber-optic probes still introduce invasion by the interface of probe and tissue and have not been proven to meet the stability or reliability requirements for long-term in vivo functionality. A potential alternative solution is to detach the probe sensing chemistry from the fiber tip, resulting in a fully-implantable luminescent sensor retained in tissue [4-6]. Furthermore, moving to micro-scale allows direct injection into skin tissue for in vivo deployment (Figure 1), much like what is commonly done for cosmetic dermal filling agents or tattoos.

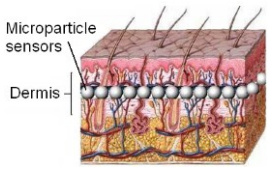

Figure 1. Scheme of dermally-implanted sensors.

R. Long is with the Department of Biomedical Engineering, Texas A&M University, College Station, TX 77843 USA. (e-mail: ruiqilong@gmail.com)

M. McShane is with the Department of Biomedical Engineering and Materials Science and Engineering Program, Texas A&M University, College Station, TX 77843 USA. (phone: 979-845-7941; fax: 979-845-4450; e-mail: mcshane@tamu.edu).

A useful implantable device must be biocompatible, must not exhibit acute reagent consumption or degradation, and must provide means of communicating the sensor output to physicians or patients. We have recently reported several different luminescent chemo-optical sensor systems that may meet the needs of implantable biochemical sensors [7-10]. So far, reaction-diffusion modeling and *in vitro* results suggest that these sensor systems can achieve adequate sensitivity, reliability, and longevity for long-term monitoring *in vivo* [10-12].

For these sensors to be deployed *in vivo*, a matched opto-electronic system for delivery of excitation, collection and analysis of escaping luminescent emission is needed. Our recent work has investigated the spectral and spatial distribution of escaping luminescence emitted from implanted sensors using 3D Monte Carlo simulation (OptiCAD® v10.033, Santa Fe, NM) . Based on the results of simulations, we designed, constructed, and evaluated the optical system, and further developed a silicone-based skin phantom to mimic optical properties of human skin as evaluation medium [13].

B. Rationale of System Optimization

However, during experiments, it was noticed that the system efficiency was compromised by the photon losses from fiber connections and the entrance aperture of the commercial CCD spectrometer, and the photon loss was greater than 99% [14]. The problem of photon loss results from an inevitable trade-off of the spectrometer. The entrance aperture and slit of most current commercial spectrometers are usually small (~hundreds microns) due to the aim of obtaining high spectral resolution and compact structure. The high resolution design results in decreased signal intensity due to the trade-off between spectral resolution and throughput. Moreover, for luminescence measurements, only specific, relatively broad bands of the spectrum are of interest. For example (Figure 2 [10, 12]), our sensors exhibit emission peaks at 585nm (FWHM≈50nm, full width at half maximum) and 645nm (FWHM≈30nm). Furthermore, luminescent signals collected from tissue or implants will be strongly attenuated by tissue scattering and absorption (~10^{-4}) [15]; therefore, signal power/system throughput should take priority over spectral resolution for luminescence.

Two optimization approaches ("two-detector system" and "customized spectral system") were proposed to solve photon loss to increase the system throughput. Experiments of two-detector system in static *in vitro* experiment showed good

SNR [14]. Previous simulation results also indicated the conceptual feasibility to design a customized high-throughput spectral system for interrogation of luminescent sensors. This paper presents the work of "customized spectral system ".

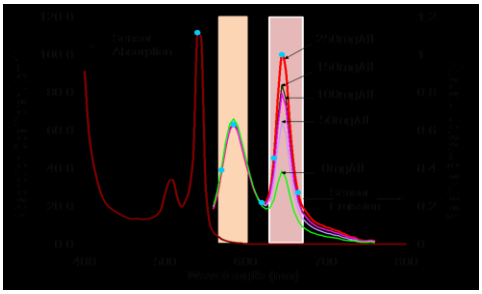

Figure 2. Excitation and emission spectra of sensor particles. For the absorption spectrum shown, [PtOEP] is 10nM.

I. Materials and Methods

A. System Design

The key to customizing the spectral system was to find a proper entrance aperture of the spectrometer system that allowed as much light input as possible into spectroscopic system while maintaining sufficient spectral resolution for our luminescent sensors (minimal: 60nm as in Figure2). As long as the system can resolve the emission peaks of the reference and sensing dyes respectively, the spectral resolution is good enough. Therefore, theoretical analysis was performed to understand the key factors and the design of a suitable system. Following the standard spectrometer design, Figure 3(a) shows the scheme of the system integrating the functions of excitation delivery, luminescence collection and spectrum measurement. Part I is the optical system to deliver excitation and collect emission light designed in previous work [16]. Part II is the layout of the customized spectrometer. The image size can be controlled by aperture size, which also controls the throughput. While aiming to achieve the minimal spectral resolution of 60nm, the aperture size, collection lenses and detector size would be optimized to optimize the system throughput, and the lenses also would be optimized to reduce system aberrations in order to optimize the system bandpass.

Figure 3(a) shows that the luminescence light escaping from skin (phantom) was collected by Part I, and it was imaged onto the entrance aperture plane on Part II. Also in Part II, the luminescence light was collimated, dispersed and finally focused onto the detector plane. Luminescence light that originated from the input focal plane of the optical system went through collimation, focusing, and again, collimation, and focusing. In reviewing this optical layout, a new possibility was conceived: it should be possible to relocate the aperture/slit from Part II to a place (as depicted in Figure 3(b)) next to the sensor/tissue. In this case, the two additional sets of focusing/collimating lenses are not needed. To investigate the effect of the position of the aperture, additional simulations were performed to compare the photons collected by the detectors.

The simulations (I and II) were performed with OptiCAD (V10.033) to compare the layouts depicted in Figure 3(a) and (b) respectively. In both groups of simulations, the power of the input excitation light was normalized to 1. In both groups of simulations, the widths of slits were 0.6, 1, 1.4, 2mm. Three phantom models with different thicknesses (268, 576, 1010μm) were used in simulations to simulate the capability of these systems when a phantom was placed on the sensors. The transparent films depicted in Figure 3 were used to collect collimated luminescence in both simulation-I and II, and the photon distributions on these two films were analyzed to compare these two designs.

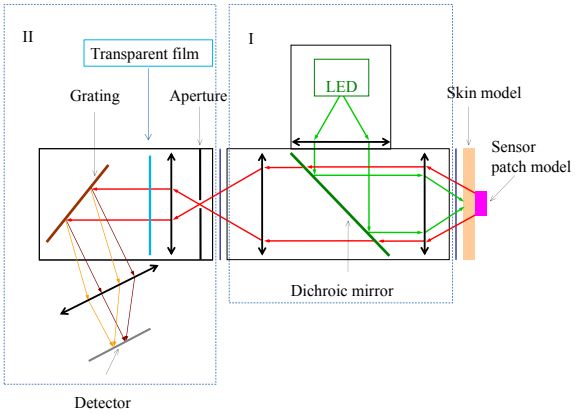

(a)

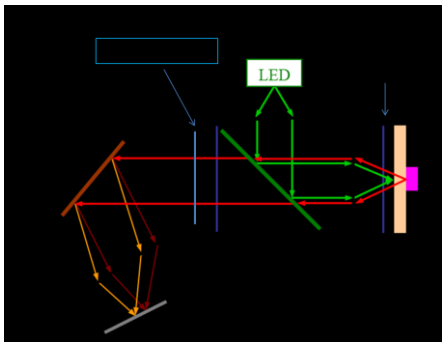

(b)

Figure 3. (a) Scheme of optimized system integrating delivery of excitation light, collection of luminescent light, and spectrum measurement. (b) Scheme of the optimization system with slit placed in front of the skin/phantom.

B. Experimental Evaluation

Experimental evaluations were performed by comparing the designed system to the bifurcated fiber bundle system previously used for in vitro and in vivo studies (NA=0.22, core=200μm, 37 excitation fibers and 41 emission fibers). The skin phantoms with different thicknesses were used for experimental evaluation. Samples were the RITC (rhodamine B isothiocyanate), and the Experimental evaluations were performed by comparing the designed system to the bifurcated mixture of PtOEP (Pt(II) octaethylporphine) and RITC solutions. A PDMS mold with a 5mm diameter hole was immobilized on a plastic petri-dish with a double-sided tape, and the sample solutions were poured into the mold. The phantoms were attached to the bottom of the petri dishes, and the excitation light was directed onto the phantoms. Two light sources (580±20nm and 645±20nm) were also used as

calibration light sources. Ocean Optics USB4000 was used to collect spectra of the bifurcated fiber bundle. The excitation light (input=17μW) with a band-pass filter (530±10nm). Integration time varied from 1ms to 500ms, and average of spectra was 2, and the number of boxcar smoothing was 15.

II. Results and Discussion

A. Simulations for Comparison of Optical Layouts

Figure 4 (a) and (b) show the integrated photon distribution on the transparent film (Figure 3) to compare the two optical layouts. The solid lines are the results of simulation (I) for Figure 3(a), and the solid circles are results of simulation (II) for Figure 3(b). In the legend, the Arabic number represented the width (mm) of the slit, and the roman numbers I and II represented different groups of simulations. Figure 4 (a) and (b) are the integrated power versus the angles to the incident normal. We can see that there is more photon power within small incident angle in simulation (II) and there is more photon power collected totally in simulation (II). The results indicate that the slit placed in front of the skin (phantom) increased the degree of collimation of luminescence photons. Moreover, the system with a slit in front of skin is simpler to construct to a more compact structure, therefore this layout in Figure 3(b) was chosen for the final design.

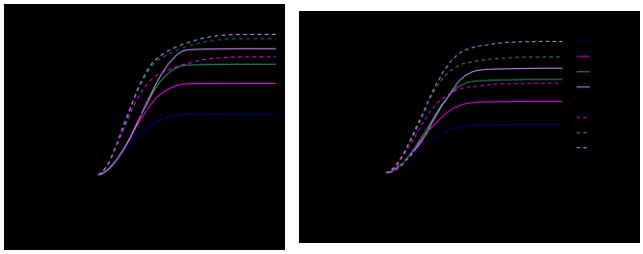

Figure 4. Integrated power of photons collected on the "transparent film"

B. Final Design

A 1mm slit was chosen for the measurement of the two peaks at 585nm and 645nm, and Figure 5 shows the simulated photon distribution on the detector. With the slit, the luminescent photons collected by this customized system are simulated to be ~100 times higher than that collected by the fiber bundle system.

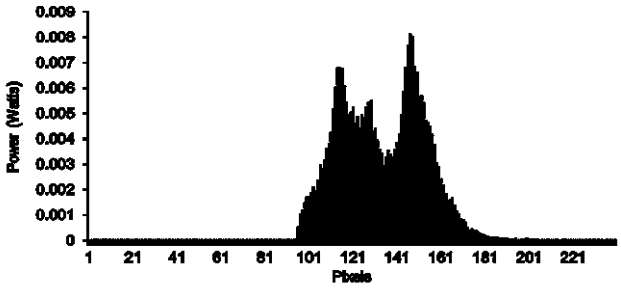

Figure 5. Simulated photon distribution of the emissions at 585 and 645nm on the detector obtained by the system with a 1mm slit.

The final design of the customized spectrometer is shown in Figure 6. The grating (NT 46-078, Edmund Optics) was ruled at 750nm with 1200/mm groove density, and the size is 30mm×30mm. The concave mirror (NT 43-470, Edmund Optics) is 50mm in diameter, and is of 50mm focal length. The detector (TCD1304AP) is from Toshiba, which is the same as the one used in Ocean optics USB4000. The half-ball lens (NT 90-860, Edmund Optics) is 8mm in diameter and of high refractive index (LaSFN9).

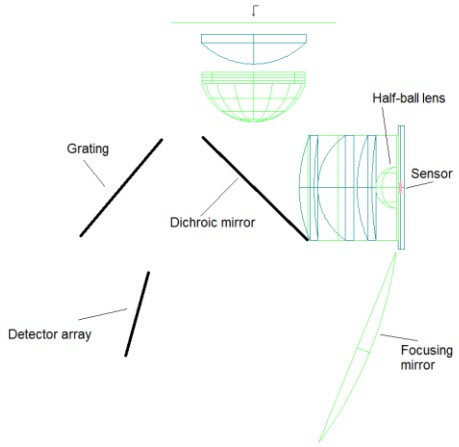

Figure 6. Final design of the customized spectral system for sensor interrogation.

C. Results of Experimental Evaluation

The comparisons of the hardware system and fiber bundle system testing results are presented in the following figures. Figure 7 is the spectra of the two light sources covered by a 1.24mm phantom, and the integration time was kept 500ms in both measurements. The peaks of the spectra obtained by the hardware system is 10 times higher than that obtained by the fiber bundle system. These measurements of the light sources aimed to compare the collection efficiency of these two systems, and the results agreed well with estimations. Because the numerical aperture (~0.8-0.9 depends on the input light source size) of the customized system is around 4 times higher than that (0.22) of the fiber bundle, and only around half of the fibers are for emission collection, thus the collection efficiency of the designed system is expected to be around 8 times higher than that of fiber bundle system.

For sensor interrogations, the efficiency of the delivery of excitation needs to be considered. Figure 8 shows the comparisons of interrogation efficiency of these two systems. When a 0.5mm phantom was attached and the integration time was kept 500ms, the photon counts of customized spectrometer were still ~100 times than that of the fiber bundle. This increase of overall interrogation efficiency of the customized system is even higher than the gain in collection efficiency. This is mainly because the delivery efficiency of the excitation light of the customized system is also higher than that of fiber bundle. The excitation light delivered by the customized system was well focused and penetrated into the skin phantom, while the excitation light delivered by fiber bundle diverged and the intensity arriving at the sensors is smaller. In contrast, a spectral trend can be detected with the customized spectrometer with should be more capable than

the fiber bundle system for in vivo measurement, in which the luminescence signal was strongly attenuated by animal skin.

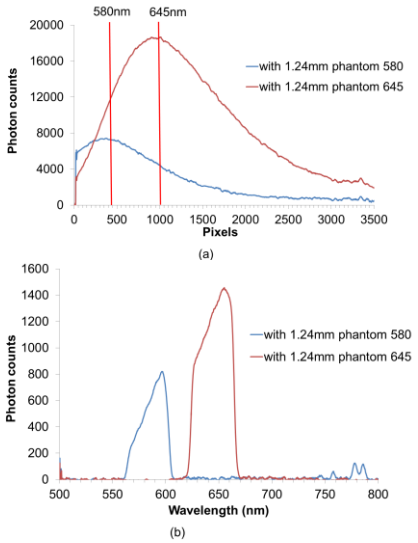

Figure 7. Spectra of the two light sources with a 1.24mm phantom covered (a) obtained from customized spectral system; (b) obtained from the fiber bundle

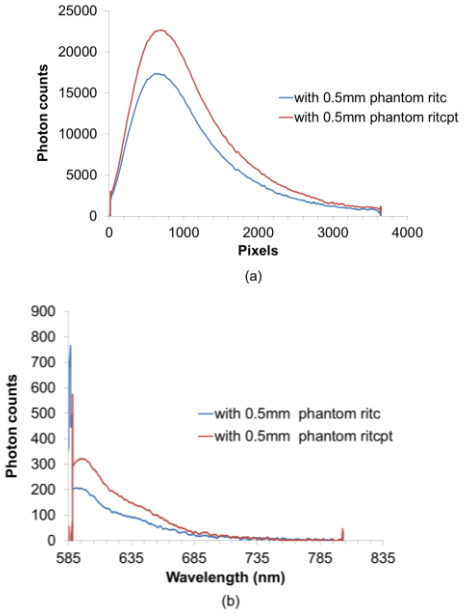

Figure 8. Spectra of the emission from RITC solutions and the mixture of RITC and PtOEP solutions (a) obtained from the customized spectral system; (b) obtained from the fiber bundle.

III. Conclusion

The customized spectral system was designed to increase the throughput while maintaining a sufficient spectral resolution. This spectral system was also cost-effective as it was 7 times less costly than the original fiber bundle and the commercial spectrometer. Compared with the two-detector system [14], the customized spectrometer is more flexible, since the two-detector system is only able to measure one specific pair of luminescence emission, if the emission peaks change, (e.g. sensors are redesigned), the filters and mirrors have to be changed. However, this system has more stray light and noise, which need to be optimized in the future. The spectral systems increased the throughput of luminescent photons while maintaining the required spectral resolution. In the future, this system can be directly coupled to an analog-to-digital converter and integrated circuits, which offers potential for a single compact and portable device for field use with luminescent diagnostic systems as well as our dermally-implanted sensors.

Acknowledgment

The authors acknowledge NIH (grant R01 EB000739), Dr. Kenith Meissner and technical support from Mr. Edward Sklar (OptiCAD®).

References

[1] R. Ballerstadt and J. S. Schultz, "A fluorescence affinity hollow fiber sensor for continuous transdermal glucose monitoring," *Anal. Chem.,* vol. 72, pp. 4185-4192, Sep. 2000.

[2] M. C. Moreno-Bondi, O. S. Wolfbeis, M. J. Leiner, and B. P. Schaffar, "Oxygen optrode for use in a fiber-optic glucose biosensor," *Anal. Chem. ,* vol. 62, pp. 2377-2380, Nov. 1990.

[3] O. S. Wolfbeis, "Fiber optic biosensing based on molecular recognition," *Sens. Actuators, B,* vol. 5, pp. 1-6, 1991.

[4] G. L. Coté, "Noninvasive and minimally-invasive optical monitoring technologies," *J. Nutr.,* vol. 131, pp. 1596S-604S, May 2001.

[5] M. J. McShane, "Potential for glucose monitoring with nanoengineered fluorescent biosensors," *Diabetes Technol. Ther.,* vol. 4, pp. 533-538, 2002.

[6] R. J. Russell, M. V. Pishko, C. C. Gefrides, M. J. McShane, and G. L. Cote, "A fluorescence-based glucose biosensor using concanavalin A and dextran encapsulated in a poly(ethylene glycol) hydrogel," *Anal. Chem.,* vol. 71, pp. 3126-3132, Aug. 1999.

[7] S. Chinnayelka and M. J. McShane, "Microcapsule biosensors using competitive binding resonance energy transfer assays based on apoenzymes," *Anal. Chem.,* vol. 77, pp. 5501-5511, Sep. 2005.

[8] P. S. Grant and M. J. McShane, "Development of multilayer fluorescent thin film chemical sensors using electrostatic self-assembly," *IEEE Sensors J. ,* vol. 3, pp. 139-146, 2003.

[9] M. J. McShane, "Microcapsule Glucose Sensors: Engineering systems with enzymes and glucose-binding sensing elements," in *Topics in Fluorescence*. vol. 10, J. R. Lakowicz and C. D. Geddes, Eds., ed New York: Springer Science, 2006.

[10] E. W. Stein, P. S. Grant, H. G. Zhu, and M. J. McShane, "Microscale enzymatic optical biosensors using mass transport limiting nanofilms. 1. Fabrication and characterization using glucose as a model analyte," *Anal. Chem.,* vol. 79, pp. 1339-1348, Feb. 2007.

[11] S. Singh and M. McShane, "Enhancing the longevity of microparticle-based glucose sensors towards 1 month continuous operation," *Biosens. Bioelectron. ,* vol. 25, pp. 1075-1081, 2009.

[12] E. W. Stein, S. Singh, and M. J. McShane, "Microscale enzymatic optical Biosensors using mass transport limiting nanofilms. 2. Response modulation by varying analyte transport properties," *Anal. Chem.,* vol. 80, pp. 1408-1417, Mar. 2008.

[13] R. Long and M. J. McShane, "Experimental Validation of an Optical System for Interrogation of Dermally-Implanted Microparticle Sensors," *Conf. Proc. IEEE Eng. Med. Biol. Soc.,* 2009.

[14] R. Q. Long and M. McShane, "High-Efficiency Optical Systems for Interrogation of Dermally-Implanted Sensors," in *Conf Proc IEEE Eng Med Biol Soc*, 2010, pp. 1033-1036.

[15] R. Long and M. McShane, "Three-dimensional, multiwavelength Monte Carlo simulations of dermally implantable luminescent sensors," *Journal of Biomedical Optics,* vol. 15, p. 027011, 2010.

[16] R. Long and M. McShane, "Optical instrument design for interrogation of dermally-implanted luminescent microparticle sensors," in *Conf. Proc. IEEE Eng. Med. Biol. Soc.*, 2008, pp. 5656-5659.